3D Digital Outcrop Model for Geological Structure Analysis in Mae Moh Coal Mine, Lampang Province, Thailand

Sangsrichan, K.,[1] Manopkawee, P.[2*] and Kanthata, S.[3]
Department of Geological Sciences, Faculty of Science, Chiang Mai University, Chiang Mai, Thailand
Email: kritsana_sangsrichan@cmu.ac.th,[1] pichawut.m@cmu.ac.th,[2*] sathit.k@cmu.ac.th[3]
**Corresponding Author*

DOI: https://doi.org/10.52939/ijg.v19i9.2847

Abstract

The advancement of unmanned aerial vehicles (UAVs) replaces traditional survey methods and provides more accurate, complete, and higher-resolution photographs than traditional aerial images. Due to the development of new surveying methods, UAVs were taken to survey the eastern Mae Moh coal mine, Mae Moh district, Lampang province, Thailand, to create a 3D digital outcrop model. Geologically, the Mae Moh coal mine forms a graben structure in which the basin's center moves downward relative to the east and west high mountains. To create the 3D model, the UAV or drone was flown over three outcrop stations to capture details of outcrops in the top and 3D views. Computer vision processing complies with aerial images from UAVs to represent bedding planes of coal seams and exposed fault characteristics. The efficiency of measuring orientations of geological structures derived from the 3D model and actual field data reveals that bedding planes and fault planes orient in a similar direction. Regarding the fault planes, the percentage error of strike ranges from 1.5% to 8.0%, whereas the percentage error of dip angle ranges between 2.4% and 2.7%. For the bedding planes, the percentage error of strike ranges from 0.5% to 10.5%, while the percentage error of dip angle ranges between 9 % and 27 %. Although the efficiency of measurements on geological structures from the 3D digital outcrop model needs to be improved, using UAVs will help develop the quality of topographic and geological surveys in the future.

Keywords: Bedding Planes, Digital Outcrop Model, Fault Planes, Mae Moh Coal Mine, Unmanned Aerial Vehicle

1. Introduction

In the field of geosciences, the representation of 2D topography strongly relies on the use of contour lines in a topographic map [1]. The topographic information can be visualized via the contours as a vertical depiction of the surface relief, providing a mental picture of the surface geometry. However, most geological features observed on the Earth's surface are not as simple as a representation of roads, rivers, or houses in a topographic map. They represent a landform where the Earth's surface interacts with the underlying Earth's subsurface. Such a complicated interaction cannot be interpreted from a cartographic topography representation on 2D maps [2].

The change of 2D representation of the surface exposure into a 3D digital model is essential for academic, industrial, and commercial applications. The digital models, known as virtual models or digital outcrop models (DOMs), offer a more realistic representation of geological features in three dimensions with less distortion and information loss [3] and [4]. The transition of 2D topographic representations into 3D digital mappings and models enables us to conduct further additional measurements, correlations, and interpretations of topographic features [5]. The advancements in survey technology have brought several methods for gathering and processing 3D models, i.e., structure-from-motion (SfM), photogrammetric survey, terrestrial light detection and ranging (Lidar), and unmanned aerial vehicles (UAVs). These techniques have expanded the accessibility of 3D data to create detailed and reasonable geological models for various disciplines in geosciences.

The use of lidar data to create 3D DOMs is decreasing due to a high investment in data collection, too many datasets for creating a small area model, and the skill requirement to process. UAVs or drone technology, the small flying vehicle that humans can remotely control, survey, and capture bird-eye views of the Earth's surface at specific locations, has been increasingly developed to replace the traditional aerial photographic survey and lidar-based methods over decades. This method provides considerable advantages of enabling access to difficult-to-reach locations while speeding up data collection and spending less laborious ground survey procedures. Moreover, the growth of UAV technology and supercomputers in making 3D models from 2D aerial photography causes a rapid improvement in digital cartography and models from UAVs, resulting in generating more accurate, complete, and up-to-date maps and 3D models [6].

Outcrops are rock bodies that have been exposed to the surface. They are a primary source of geological information for studies and research. The exposure of rock provides observation for geological analysis, creating geologic maps, geological history, and exploration of mineral resources. Traditional field mapping techniques have remained significantly unchanged in several places worldwide, causing the limitation of quantitative measurements on rock structures, a lack of description of the lateral continuity of rock layers, and an incomplete spatial expression of topographic features at a large scale. Using 3D DOMs generated by UAVs can solve these problems obtained from traditional field mapping methods.

Some early models were successful in using UAVs to create 3D DOMs. The 3D mapping generates a meter-scale model of complex carbonate structures that could elaborate facies architecture and heterogeneity along inaccessible faces of the quarry [7]. UAVs provide a precise model of outcrop exposures from different perspectives without carrying heavy tools and equipment. Moreover, a DOM generated from the UAVs was used to survey extensive exposures of Late Cretaceous fluvially stratigraphic outcrops without requiring specialized hardware and software. The study site's geological history can be interpreted based on the 3D DOM with the detail of the stratigraphic distribution of dipping floodplain mudstone beds interbedded with sandstone channel deposits [8]. Furthermore, the UAVs can create a DOM for structural analysis in the Permian Khao Luak Formation, Phetchabun, Thailand, to illustrate the orientations of rock and bed thickness with an acceptable accuracy and resolution for measurement [9].

Mae Moh coal mine covers a 135 km^2 lignite mine in Mae Moh sub-district, Mae Moh district, Lampang province, Thailand (Figure 1). EGAT (Electricity Generating Authority of Thailand) operates this mine, which has a production capacity of 16 million tons of lignite per year [10]. Layers of coal seams are primarily found in the Na Khaem Formation in a stratigraphic column of the Mae Moh Group [11]. In general, the amount of coal resources is based on the areal extent of the coal seams, the thickness of the coal seams, and in situ density [12]. However, an assessment of the overall extent of coal seams is mainly based on traditional field observation and measurements for surficial coal exposures. Some of those layers may be in far and inaccessible areas. This study focuses on the preliminary investigation of 3D mapping, measurement, and analysis of surficial coal exposures in the Mae Moh coal mine, where outcrops can be measured from UAVs and field observations. The objectives of the study are to construct 3D DOMs that quantitatively enable measurements of geological structures and orientations of coal seams in an outcrop-scale perspective that was previously challenging to achieve with traditional field methods, and to compare the performance of data collection between field-based and UAV-based measurements.

2. Geological Background of the Study Site

Mae Moh coal mine is a part of the oval-shaped Mae Moh Basin that trends in the NNE-SSW direction. The elevation of the basin is approximately 330 m above sea level. Steep and sub-parallel mountains in the basin, which are underlain by the Triassic rock of the Lampang group, including limestone, shale, and sandstone (TRpt, TRpk, TRhh, TRdl, TRpd), are situated on the eastern and western sides of the basin (Figure 2(a)). The steep mountains are associated with N-S striking normal faults that have resulted from the extension of the tectonic regime since the Tertiary. Thinly unconsolidated fluvial deposits and alluvium mantle the central basin. The layers of the coal seams underneath the basin emerge throughout the basin [13]. The Tertiary succession in the Mae Moh basin is called the Mae Moh Group (Tmm), which is composed of [11] [14] and [15].

Huai King Formation: The lowermost formation of the Mae Moh Group consists of semi-consolidated clastic sedimentary rock ranging from conglomerate at the base to mudstone/ claystone on top. Na Khaem Formation: The coal-bearing formation. Mudstone consists of fossils, burrows, and borings. Its thickness is 250-400 m.

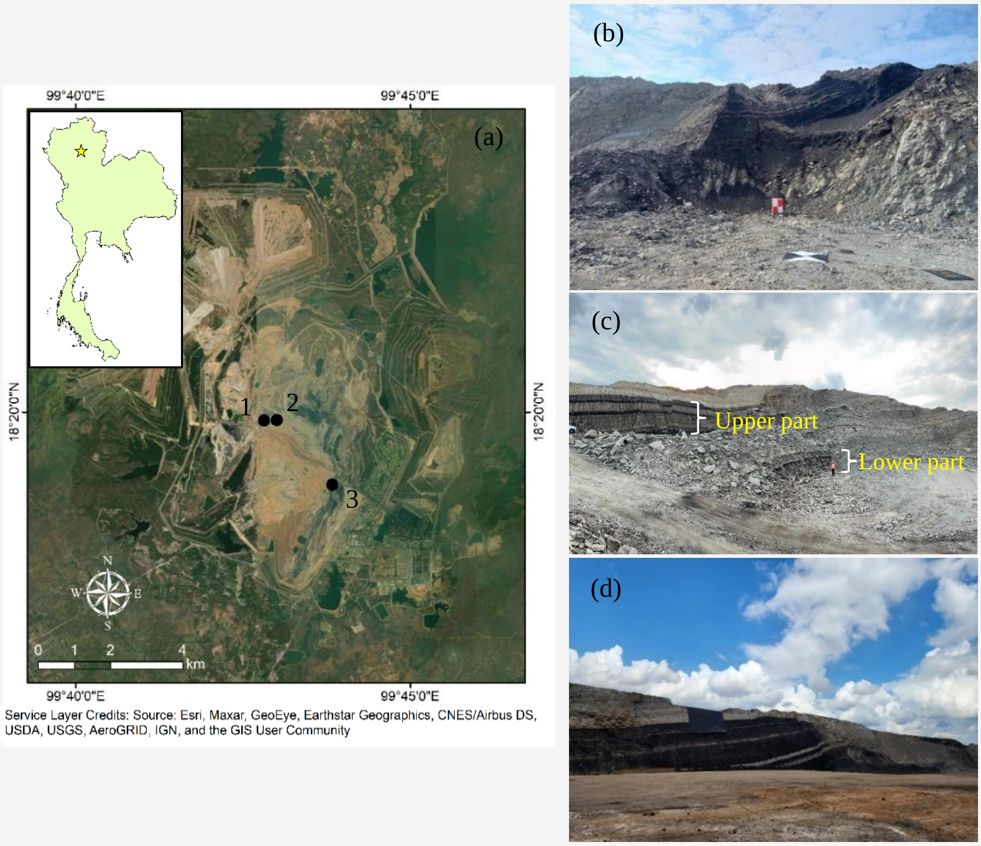

Figure 1: (a) Topographic settings of Mae Moh coal mine, Mae Moh district, Lampang, Thailand. The inset illustrates the location of the Mae Moh coal mine (yellow star) in northern Thailand. Numbers depict the study sites of the outcrop surveys (b) The first site (c) The second site (d) The third site

The lignite zone interbeds with mudstone called J-seam, K-seam, and Q-seam. Huai Luang Formation: The semi-consolidated and unconsolidated sediments mainly comprise fine-grained sedimentary rock with the lens of coarse-grained clastic rock in the basin's center. This rock formation is red-brown due to the oxidation of fine-grained pyrite in the layers (Figure 2(b)).

The study sites to capture the geological structures of coal seams in the Mae Moh coal mine are three surveyed sites in the middle of the Mae Moh coal mine. These sites expose outcrops where coal seams are horizontally aligned and faulted.

3. Methodology

The study starts with capturing aerial images over the study sites by UAV, computer vision processing through 1) the Agisoft Metashape Professional (AMP) software to generate the 3D DOMs and export them onto the real-world coordinates, and 2) the Virtual Reality Geological Studio (VRGS) software to compare orientations (strike, dip angle, and dip direction) of bedding planes and fault planes between field and software measurements.

3.1 Field Data Acquisition

The photogrammetric technique is the main principle that requires photographs gathered from various sources, including the UAV equipped with a high-resolution camera and the ground-based digital camera with built-in GPS. Here, the DJI Phantom4 Pro V2.0 UAV, owned by the Department of Geological Sciences, Chiang Mai University, was used to capture outcrop-scaled geological structures. The field staff in the Mine Survey section of the Mae Moh coal mine flew the WingtraOne to survey large-scale rock exposure over the study site. The settings of the three sites that the UAVs surveyed were:

- The first site is located at 18.33134, 99.713574, where the elevation of the outcrop is 260 m above sea level, and the height of the outcrop is 20 m (Figure 1(b)).
- The second site is located at 18.331426, 99.716739, where the elevation of the outcrop is 311 m above sea level, and the height of the lower

ISSN: 1686-6576 (Printed) | ISSN 2673-0014 (Online) |

and upper parts of the outcrop is 15 m and 25 m, respectively (Figure 1(c)).

- The third site is located at 18.315570, 99.730578, where the elevation of the outcrop is 302 m above sea level, and the height of the outcrop is 35 m (Figure 1(d)).

The ground control point (GCP) is a well-defined point on the Earth's surface that is used as a reference point in mapping, modeling, and photogrammetric applications. Coordinates of the three GCPs at each study site were acquired over an 80-cm invented red scale cube, and two 60-cm black and white GCPs using a real-time kinematic (RTK) survey method. The precise coordinates were used to reference the coordinate system in a real-world situation. High overlap between the images and the different perspectives between air and ground must be determined to receive accurate results.

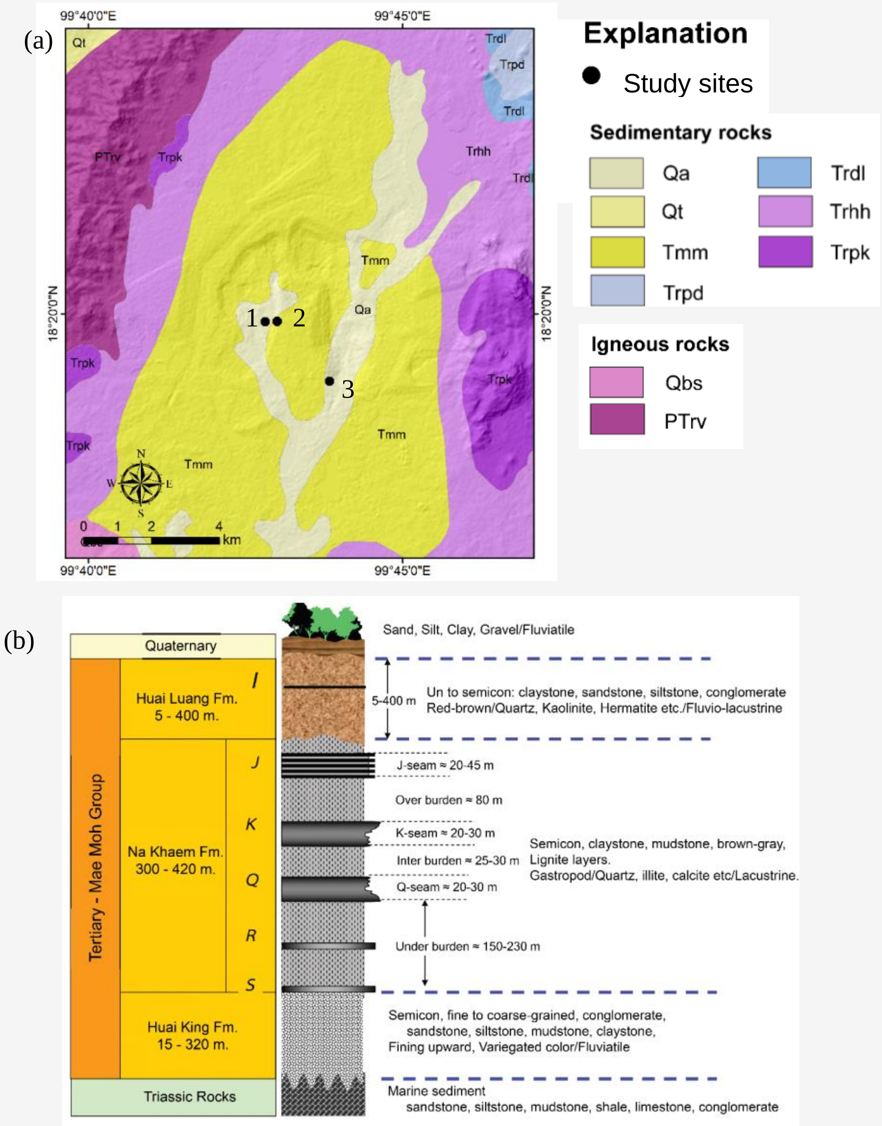

Figure 2: (a) Geological setting of Mae Moh coal mine (modified from [16]). Abbreviation of geological formations; Qa: Quaternary alluvial sediment, Qt: Quaternary alluvial terraces, Tmm: Tertiary Mae Moh semi-consolidated and unconsolidated sediments with a coal-bearing formation of five zones of lignite, Trpd: Triassic Pha Daeng formation, Trdl: Triassic Doi Long formation, Trhh: Triassic Hong Hoi formation, Trpk: Triassic Pha Kan formation, Qbs: Quaternary basalt, and PTrv: Permo-Triassic volcanic rock. Numbers depict the study sites of the outcrop surveys. (b) Stratigraphic column of Mae Moh basin (modified from [17] and [18])

ISSN: 1686-6576 (Printed) | ISSN 2673-0014 (Online) | © Geoinformatics International

Using a regular grid survey pattern, the UAV was flown to capture images that forward overlap around 60-70% in the flight path direction and 25-40% side overlap [19]. For the first flight, the WingtraOne was flown at an altitude of 100 m with the ground sampling distance (GSD) at 1.57 cm/pixel. It was flown as single grid and circular surveys over the first and second sites in a north-south flight direction and the third site in an east-west direction in order to capture the overview of the study site without very detailed results. The DJI Phantom4 Pro V2.0 UAV was flown for the second flight using a double grid survey to capture detailed geological structures (Figure 3). The flight direction was both north-south and east-west directions. The camera angle was fixed at 60^{o}, and the flight was lowered to the altitude of 50 m with 1.36 cm/pixel of GSD. This flight operation gave us a single image footprint on the ground at approximately 75 m wide [20]. Apart from the UAV survey, the orientations of bedding planes of coal seams and fault planes exposed to the surface were measured, and their coordinates were collected during the fieldwork (Figure 4).

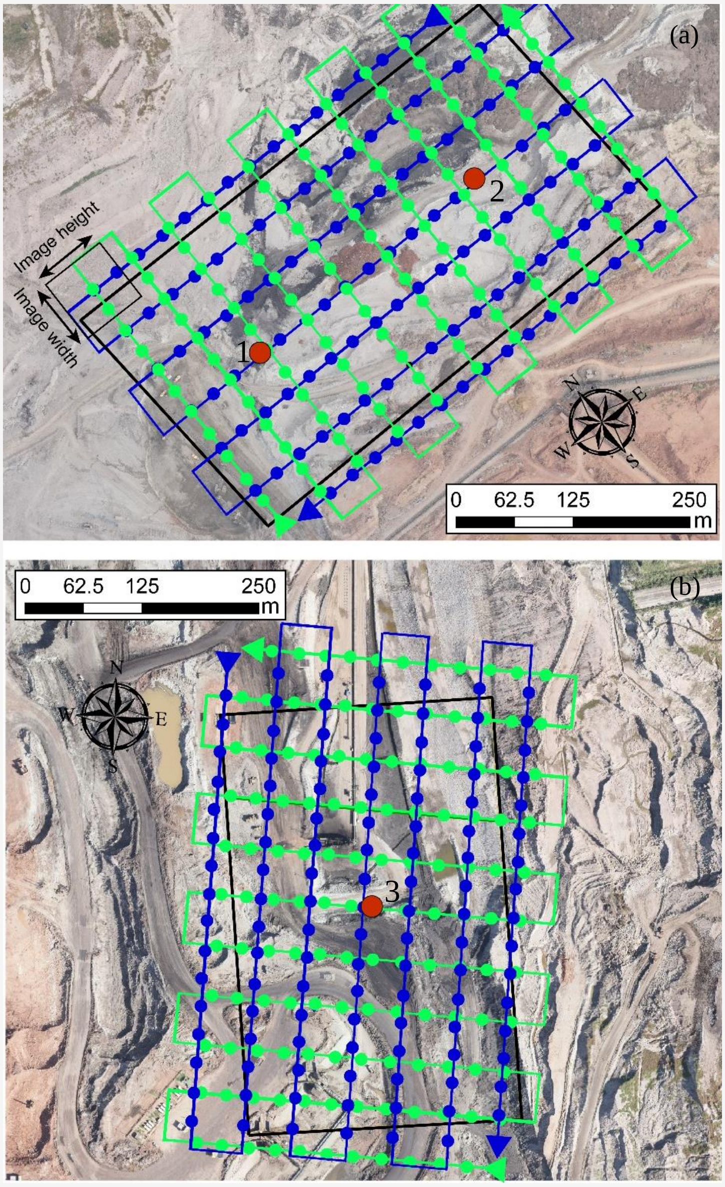

Figure 3: Double grid of the UAV flight paths (blue and green lines) with sample images (blue and green dots). Black rectangles represent the areas to create the 3D DOMs. **(**a) Flight paths over the first and second sites (b) Flight paths over the third site (modified from [21])

ISSN: 1686-6576 (Printed) | ISSN 2673-0014 (Online) | © Geoinformatics International

Figure 4: Measurement of the orientation of bedding planes of coal seams and fault planes.
(a) The first site (b) The lower part of the second site (c) The upper part of the second site (d) The third site

3.2 Computer Vision Processing

Images of rock outcrops obtained from the UAV were imported into the AMP. Most images were georeferenced with coordinates (latitude, longitude) and altitude because the latest UAVs and cameras have built-in GPS tagging options. In the case of some images lacking coordinates, the AMP helped us to analyze the object shown in the image to match the same object in the adjacent images. The matching of images depends on the alignment and orientation of the cameras toward the targets. Then, the object and the image that contains the object were automatically georeferenced. Some geological structures' coordinates were additionally collected during the fieldwork with a portable GPS to tie the object to the coordinate system.

The project coordinate system was set according to the projection datum of the area. The AMP aligned the common points shown among sequentially captured images in the direction of the UAV's flights with the World Geographic System 1984 (WGS1984) and UTM zone 47Q. The program automatically generated point clouds when those images were aligned. Moreover, the AMP allowed us to rebuild dense point clouds to provide more details on point clouds' distances, positions, colors, and textures. This step also interpolated available point clouds into the gap and removed anomalies on the irregular surface topography [22]. The denser the point clouds, the more effective the AMP is to construct a triangular mesh over those dense point clouds and a textured mesh to create 3D DOMs for the three study sites. Eventually, these 3D DOMs were exported into a readable format in Google Earth Pro to verify the accuracy of point clouds' coordinates and altitude onto the real-world coordinates [23].

3.3 Measurements of Geological Structures and Outcrop Orientations

Because the 3D DOMs are an orthophotograph that represents the Earth's surface and can be used to measure actual angles on the geological structures and exposed outcrops, the model was transferred into the VRGS to create several virtual bedding planes along coal seams and fault planes. Once the north direction was specified for the model, this software automatically measured the dip angle and dip direction of rocks and fault planes. The dip direction of the planes was converted into a strike of the rock layers and fault planes at 90^{o} ahead or behind the dip direction.

3.4 Efficiency Comparison between Field Data and 3D DOMs

The percentage error was determined to compare the efficiency of the measurement of geological structures from field data and 3D DOMs. The percentage error is the difference between the observed angle and the actual angle in comparison to the actual angle as expressed in equations 1 to 3 [24]:

$$Absolute\ Error = V_0 - V_a$$

Equation 1

$$Relative\ Error = \frac{V_0 - V_a}{V_a}$$

Equation 2

$$Percentage\ Error = \frac{[V_0 - V_a]}{V_a} \times 100$$

Equation 3

where:

PE is percentage error

V_0 is an observed angle of strike and dip obtained by software

V_a is an actual angle of strike and dip measured in the field

4. Results

4.1 3D Digital Outcrop Models

A representative view of the 3D DOMs represents the top and 3D views of the three surveyed outcrops in the Mae Moh coal mine (Figures 5, 6, 7). The first model covers approximately 625 m^2, representing the exposed coal seam layer in the middle of the model (47Q 575400E 2026992N). The rest of the model shows the layered sediment covering the coal seam (Figure 5). This second model covers 2,000 m^2, including the total lower and upper parts of the outcrop in the southeast. The thick sediment covers the south-southwest side of the model. The lower part is approximately 15 m high, measured from the base to the excavated overburden. The upper part is about 25 m high. This upper part exposes some coal seam layers with a small fault line (47Q 575734E 2027002N) (Figure 6). The third model includes approximately 2,250 m^2, representing the thick coal seam layer of the 25-m-heigh outcrop and the semi-mobile sizing station in the middle of the model (47Q 577203E 2025254N). The northwestern side of the model is covered with overburdened sediment (Figure 7). For structure modeling and analysis, the variations of coal seam thickness and structures can be observed from these models, allowing us to measure the outcrop's bedding planes and fault planes.

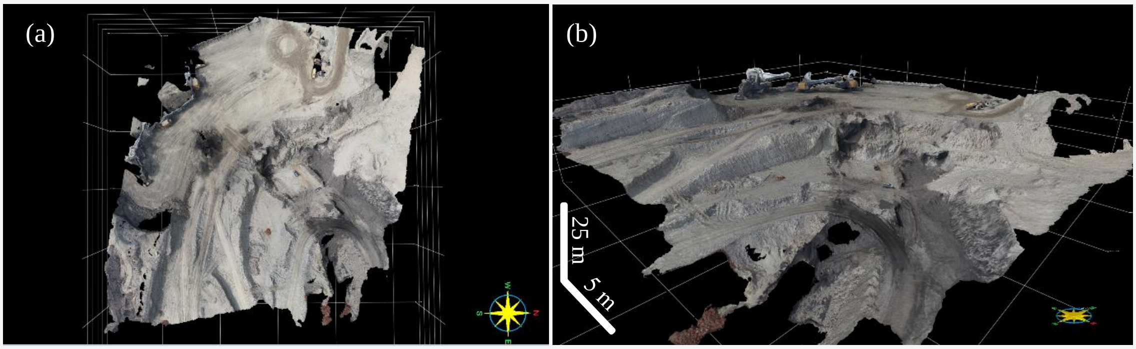

Figure 5: Images show the 3D DOM of the first site in (a) Top view (b) 3D view

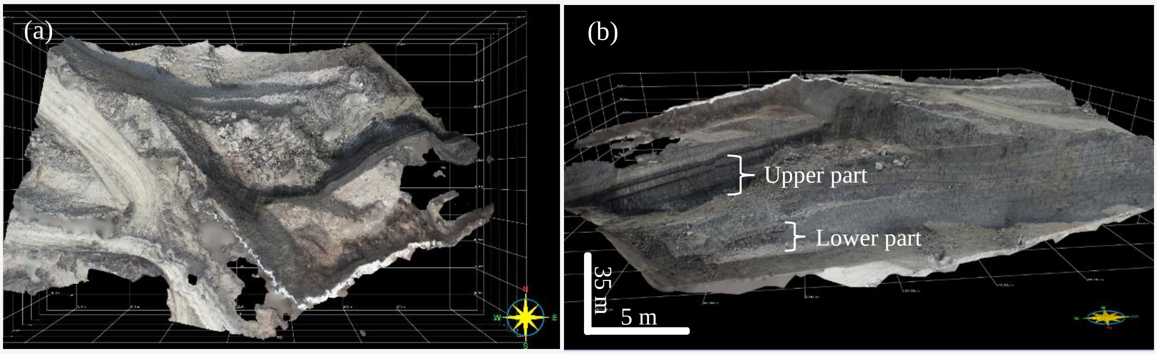

Figure 6: Images show the 3D DOM of the second site in (a) Top view (b) 3D view

ISSN: 1686-6576 (Printed) | ISSN 2673-0014 (Online) | © Geoinformatics International

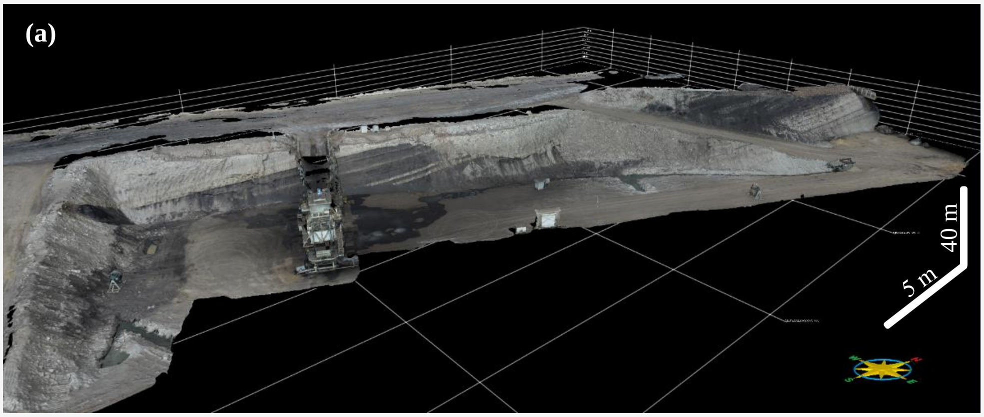

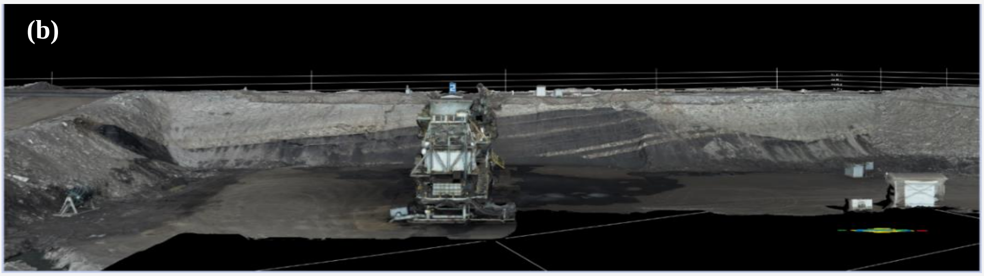

Figure 7: Images show the 3D DOM of the third site in 3D view

4.2 Efficiency Comparison of Geological Structures between Field Data and 3D Digital Outcrop Models

The measurement efficiency of two geological structures (strike and dip angle of coal seams and fault planes) derived from field data derived from field data was compared to those obtained from the 3D DOMs. The locations to measure bedding planes and fault planes in each site are shown in Figure 8. The average orientations of the fault planes and the percentage error (PE) are shown in Table 1. The average orientations of the bedding planes of coal seams and the percentage error (PE) are demonstrated in Table 2. The measurement of orientations and dip angle of fault planes reveals that:

- The average orientations of the fault planes in the first site measured in the field and the models are at 208°/80°SE and 204°/82°SE, respectively. The PE of the strike is 1.9%, and the dip angle is 2.5%.

- The outcrop in the second site was separated into the lower and upper parts. The average orientations of the fault planes in the lower part measured in the field and the models are 136°/37°NE and 147°/37°NE, respectively. The PE of the strike is 8.1%, and no PE of the measured dip angle. The average orientations of the fault planes in the upper part measured in the field and the models are 195°/41°NW and 192°/42°NW, respectively. The PE of the strike is 1.5%, and the dip angle is 2.4%.

- The fault plane curve (the listric normal fault) in the third site creates high uncertainty in the measurement of the orientation of the fault plane. Thus, there is no measurement of fault plane orientation.

The measurement of orientations and dip angle of bedding planes of coal seams represents that:

- The average orientations of the bedding planes in the first site measured in the field and the models are 287°/55°NE and 257°/60°SE, respectively. The PE of the strike is 10.5%, and the dip angle is 9.1%.

- The lower part of the outcrop in the second site shows the average orientations of the bedding planes measured in the field and the models at 259°/20°NE and 266°/18°NE, respectively. The PE of the strike is 2.7%, and the dip angle is 10%. The upper part depicts the average orientations of the bedding planes measured in the field and the models at 239°/18°NE and 227°/23°NE, respectively. The PE of the strike is 5%, and the dip angle is 27.8%.

- The average orientations of the bedding planes in the third site measured in the field and the models are 191°/33°NW and 190°/37°NW, respectively. The PE of the strike is 0.5%, and the dip angle is 12%.

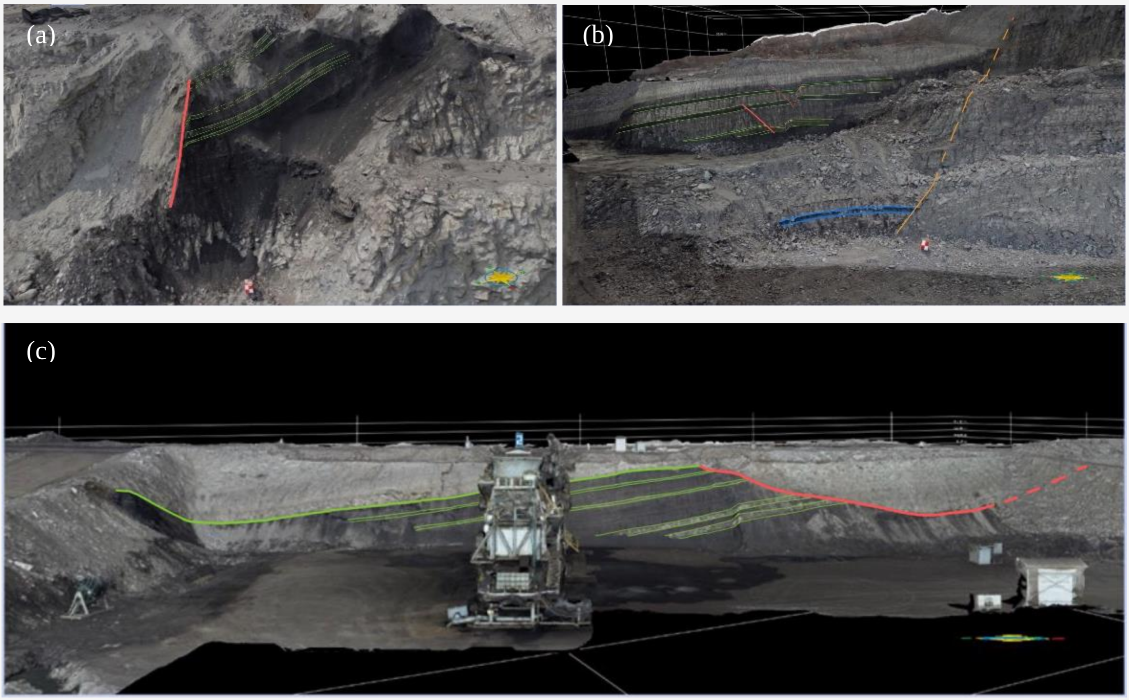

Figure 8: Bedding planes and fault planes measurement in each site. Green and blue lines represent bedding planes, and red and orange lines represent fault planes. (a) The first site (b) The second site (c) The third site

Table 1: The comparison of the orientations of fault planes between field measurement and 3D DOMs and the percentage error

Site \ orientations	Field measurement	3D DOMs	PE_{Strkie} (%)	PE_{dip} (%)
1	208°/80°SE	204°/82°SE	1.9	2.5
2 (lower)	136°/37°NE	147°/37°NE	8.1	0
2 (upper)	195°/41°NW	192°/42°NW	1.5	2.4
3*	-	-	-	-

** No measurement of orientation of fault planes in the third site due to a curved fault*

Table 2: The comparison of the orientations of coal seam bedding planes between field measurement and 3D DOMs and the percentage error

Site \ orientations	Field measurement	3D DOMs	PE_{Strkie}(%)	PE_{dip}(%)
1	287°/55°NE	257°/60°SE	10.5	9.1
2 (lower)	259 °/20°NE	266°/18°NE	2.7	10
2 (upper)	239°/18°NE	227°/23°NE	5	27.8
3	191°/33 °NW	190°/37°NW	0.5	12

5. Discussion

The collision between the Indian and Eurasia plates in the Eocene or 45 million years ago developed substantial continental block movement, rotation, and strike-slip faults that created the rhomb-shaped Mae Moh basin [25]. The later uplift across northern Thailand caused the Mae Moh basin to erosional processes and coal seam exposures. Most coal seam outcrops exposed throughout the Mae Moh coal mine are lignite deposits in the Na Khaem formation of the Mae Moh Group [26]. The UAV was conducted to capture the coal seam bedding planes that are planar and semi-curved planar. The 3D DOMs created by overlapping aerial images from the UAV and the WingtraOne can capture the overview of the study site and detailed geological structures in the three surveyed sites. The high-resolution images make us observe bedding planes and fault planes. Remarkably, the 3D DOM from the third site captures the outcrop's front and side views. Hence, the strike of bedding planes and the actual dip angle were efficiently measured. Likewise, the 3D DOM from the second site shows the hanging wall moving down relative to the footwall.

Based on the geological structures' orientations in the three surveyed sites that are measured during the fieldwork and processed through the 3D DOMs (Table 1 and Table 2), the percentage error of strikes of the fault plane is low in the first outcrop and the upper part of the second outcrop because the exposure of fault offset makes it easy to create and measure virtual planes. However, a listric normal fault in the third site makes measuring its strike difficult. Thus, this study does not measure the orientation of this fault plane. Regarding the bedding planes of the coal seams, all strikes, dips, and dip directions vary between the two methods. Nonetheless, the percentage error of orientations of coal seams' bedding planes is higher than the fault plane's orientations. This high percentage error may be due to the spatial variation of the position of bedding planes to be measured. Moreover, the curved contact of bedding planes with overlain unconsolidated sediment causes a challenging measurement of the orientations on the virtual planes. Although the efficiency of measurements on geological structures from the 3D DOMs could be higher, this study can provide insight into how these models will improve the quality of topographic and geological surveys.

When comparing the efficiency of the UAV-based measurement approach with the traditional field method, it is important to note that processing images obtained from the UAV can be time-consuming, especially on a computer lacking a graphic processing unit (GPU). Furthermore, effectively utilizing the UAV-based approach necessitates using additional software tools. More field data and outcrops are sometimes needed in order to represent details on geological structures at local- and regional-scale models. Although the UAV survey has proven to provide a less-tedious, cost-effective, safer, and more efficient survey over larger areas in various environments, this method still demands specialized and experienced users rather than typical geologists. Our study still recommends combining traditional and UAV-based surveys to enhance the efficiency and accuracy of field data collection.

6. Conclusion

The 3D digital outcrop models derived from unmanned aerial vehicles are used to analyze geological structures in the Mae Moh coal mine, Mae Moh district, Lampang province, Thailand. The method starts with compiling aerial photography from unmanned aerial vehicles to create 3D digital outcrop models and quantify the orientations of fault planes and bedding planes of coal seams. Our results reveal that bedding planes of coal seams and fault planes obtained from the field and the 3D digital outcrop models are comparable. The percentage error of measuring bedding planes is higher than fault planes because of the spatial variation in bedding planes' measured position and shape. Thus, combining fieldwork with 3D digital outcrop models will provide better results than the dependence on 3D digital outcrop models alone.

The 3D digital outcrop models can support stratigraphic and fault orientation data in inaccessible areas. In the future, the model will help create a cross-sectional profile in the Mae Moh coal mine and provide more detailed and accurate geological data. Our research highlights the 3D digital outcrop model as a necessary tool for geological surveys and research in the future.

Acknowledgement

The authors would like to express our gratitude to Asst. Prof. Dr. Weerapan Srichan, a head of the Department of Geological Sciences, Chiang Mai University, for his efforts and coordination in requesting access to the Mae Moh coal mine. The authors highly appreciate the preliminary review of the manuscript from Asst. Prof. Dr. Kannipa Motanated from the Department of Geological Sciences, Chiang Mai University. The authors also appreciate the advice in creating digital outcrop modeling in the Agisoft Metashape Professional and Virtual Reality Geological Studio software from Asst. Prof. Dr. Sukonmeth Jitmahantakul, Department of Geology, Chulalongkorn University, and Asst. Prof. Dr. Phonpat Hemwan, Department of Geography, Chiang Mai University. The authors want to thank Mr. Prachuap Donkammoon, an assistant governor of the Mae Moh coal mine, Mr. Teeradon Thongkham from the Mine Survey Section, Mr. Wasawat Saisingthong and Mr. Pichet Kaewsomwang from the Geology Section in the Mae Moh coal mine for logistics between sites and outcrops, WingtraOne operations, and essential information about the Mae Moh coal mine, and Mr. Siwakorn Maneethien, an undergraduate student, for the field assistance. Many thanks should be given to the 50th Anniversary Geology Fund that financially supported this research project. Finally, the authors acknowledge anonymous reviewers' critical comments and suggestions to improve the manuscript significantly.

References

[1] Hutton, C., (1778). An Account of the Calculations Made from the Survey and Measures taken at Schehallien, in Order to Ascertain the Mean Density of the Earth. *Philosophical Transactions of the Royal Society of London*, Vol. 68, 756-757. https://doi.org/10.1098/rstl.1778.0034.

[2] Bond, C. and Wightman, R., (2012). Beyond Map View: Teaching the Conceptualisation and Visualisation of Geology through 3D and 4D Geological Models. *Planet*, Vol. 25(1), 7-15. https://doi.org/10.11120/plan.2012.00250007.

[3] McCaffrey, K. J. W., Jones, R. R., Holdsworth, R. E., Wilson, R. W., Clegg, P., Imber, J., Holliman, N. and Trinks, I., (2005). Unlocking the Spatial Dimension: Digital Technologies and the Future of Geoscience Fieldwork. *Journal of Geological Society*, Vol. 162(6), 927-938. https://doi.org/10.1144/0016-764905-017.

[4] Jones, R., McCaffrey, K., Clegg, P., Wilson, R., Holliman, N., Holdsworth, R., Imber, J. and Waggott, S. (2009). Integration of Regional to Outcrop Digital Data: 3D Visualisation of Multi-Scale Geological Models. *Computer & Geosciences*, Vol. 35, 4-18. https://doi.org/10.1016/j.cageo.2007.09.007.

[5] Nesbit, P. R., Durkin, P. R., Hugenholtz, C. H., Hubbard, S. M. and Kucharczyk, M., (2018). 3-D Stratigraphic Mapping Using a Digital Outcrop Model Derived from UAV Images and Structure-from-Motion Photogrammetry. *Geosphere*, Vol. 14(6), 1-18. https://doi.org/10.1130/GES01688.1.

[6] Carrera-Hernamdez, J. J., Levresse, G. and Lacan, P., (2020). Is UAV-SfM Surveying Ready to Replace Traditional Surveying Techniques? *International Journal of Remote Sensing*, Vol. 41(12), 4820-4837. https://doi.org/10.1080/01431161.2020.1727049.

[7] Thomas, H., Brigaud, B., Blaise, T., Saint-Bezar, B., Zordan, E., Zeyen, H., Andrieu, S., Vincent, B., Chirol, H., Portier, E. and Mouche, E., (2021). Contribution of Drone Photogrammetry to 3D Outcrop Modeling of Facies, Porosity, and Permeability Heterogeneities in Carbonate Reservoir (Paris Basin, Middle Jurassic). *Marine and Petroleum Geology*, Vol. 123. https://doi.org/10.1016/j.marpetgeo.2020.104772.

[8] Nesbit, P. R., Boulding, A. D., Hugenholtz, C. H., Durkin, P. R. and Hubbard, S. M., (2020). Visualization and sharing of 3D Digital Outcrop Models to Promote Open Science. *GSA Today*, Vol. 30(6), 4-10. https://doi.org/10.1130/GSATG425A.1.

[9] Phetheet, J., Lhosupasirirat, K., Panyapradit, T., Jirarachwaro, S. and Jitmahantakul, S., (2016). A New Technique for Making Digital Outcrop Model for Structural Analysis: An Example from the Permian Khao Luak Formation outcrop in Phetchabun, Thailand. *International Conference on the Tectonics of the Northwestern Indochina (TNI-2016)*, February 22-24, 2016, Chiang Mai, Thailand.

[10] Praiwan, Y., (2018). EGAT to Propose Coal Plant Upgrade. *Bangkok Post*, October 2, 2018 [Online]. Available: https://www.bangkokpost.com/business/1550310/egat-to-propose-coal-plant-upgrade.

[11] Songtham, W., Ugai, H., Imsamut, S., Maranate, S., Tansathien, W., Meesook, A. and Saengsrichan, W., (2005). Middle Miocene Molluscan Assemblages in Mae Moh Basin, Lampang Province, Northern Thailand. *ScienceAsia*, Vol. 31, 183-191. https://doi.org/10.2306/scienceasia1513-1874.2005.31.183.

[12] Coalfields Geology Council of New South Wales and the Queensland Mining Council, (2001). Guidelines for the Estimation and Reporting of Australian Black Coal Resources and Reserves. *Joint Ore Reserves Committee Code (‘The JORC Code’) 1999 Edition*, [Online]. Available: https://www.jorc.org/docs/coalguidelines2001.pdf.

[13] Bunopas, S., (1982). Paleographic History of Western Thailand and Adjacent Parts of Southeast Asia-a Plate Tectonics Interpretation. *Geological Survey Paper, Royal Thai Department of Mineral Resources, Thailand*, Vol. 5, 1-810.

[14] Ward, C. R., (1991). Mineral Matter in Low-Rank Coals and Associated Strata of the Mae Moh Basin, Northern Thailand. *International Journal of Coal Geology*, Vol. 17, 69-93. https://doi.org/10.1016/0166-5162(91)90005-4.

[15] Vichiadid, T., Soodprasert, T., Sastri, N., Oopathum, C. and Limsuwan, P. (2008). Determination of U, Th and K in Sediments and Fossil Collected from Mae Moh Mine Using Gamma-Ray Spectrometry and Neutron Activation Analysis (NAA). *Kasetsart Journal (Natural Science)*, Vol. 42, 333-339. https://li01.tci-thaijo.org/index.php/anres/article/view/244616.

[16] Geological Survey Division, (1995). Geological Map of Changwat Lampang NE47-7 Scale 1:250,000. *Geological Survey Division, Department of Mineral Resources*, Bangkok, Thailand.

[17] Doncommul, P., Pimklang, P., Mungpayabal, N. and Chaiwan, A. (2011). Reviews of Slope Failure in Lowwall Area 3 of Mae Moh Mine. *Rock Mechanics, Fuenkajorn and Phien-wej (Eds)*, 219-227.

[18] Zarlin, N., Sasaoka, T., Shimada, H. and Matsui, K. (2012). Numerical Study on an Applicable Underground Mining Method for Soft Extra-Thick Coal Seams in Thailand. *Engineering*, Vol. 4, 739-745. https://doi.org/10.4236/eng.2012.411095.

[19] Falkner, E. and Morgan, D., (2001). *Aerial Mapping: Methods and Applications*, 2nd ed. Boca Raton, FL: CRC Press, 2001. Available: https://doi.org/10.1201/9780367801359.

[20] Leachtenauer, J. C. and Driggers, R. G., (2001). *Surveillance and Reconnaissance Image Systems: Modeling and Performance Prediction*. Artech House: Norwoord, MA, USA.

[21] Pessacg, F., Gómez-Fernández, F., Nitsche, M., Chamo, N., Torrella, S., Ginzburg, R. and De Cristóforis, P., (2022). Simplifying UAV-Based Photogrammetry in Forest: How to Generate Accurate Digital Terrain Model and Access Flight Mission Settings. *Forests*, Vol. 13(2). https://doi.org/10.3390/f13020173.

[22] Parra, H. and Gomes, J., (2017). Integrated Workflow for Building 3D Digital Outcrop Models using Unmanned Aerial Vehicles-Drones: Field Case Thamama Group, Wadih Rahbah, UAE. *Proceeding of the Abu Dhabi International Petroleum Exhibition & Conference, Abu Dhabi, UAE, November, 2017*, https://doi.org/10.2118/188477-MS.

[23] Tavani, S., Granado, P., Corradetti, A., Girundo, M., Iannace, A., Arbués, P., Muñoz, J. A. and Mazzoli, S., (2014). Building a Virtual Outcrop, Extracting Geological Information from it, and Sharing the Results in Google Earth via OpenPlot and PhotoScan: An Example from the Khaviz Anticline (Iran). *Computer & Geosciences*, Vol. 63, 44-53. https://doi.org/10.1016/j.cageo.2013.10.013.

[24] Wu, G., Baraldo, M. and Furlanut, M., (1995). Calculating Percentage Prediction Error: A User's Note. Pharmacological Research, Vol. 32(4), 241-248.

[25] Johnson, B. D., Powell, C. McA. and Veevers, J.J. (1976). Spreading History of the Eastern Indian Ocean and Greater India's Northwest flight from Antarctica and Australia. *Geological Society of America Bulletin*. Vol. 87, 1560-1566. https://doi.org/10.1130/0016-7606(1976)87%3C1560:SHOTEI%3E2.0.CO;2.

[26] Ratanasthien, B., Takayasu, K., Fyfe, W. S., Kandharosa, W. and Kusakabe, M., (2004). Sulfer Isotopic Implication of Middle Miocene Marine Incursion in Northern Thailand. *ScienceAsia*, Vol. 30, 43-58. https://www.thaiscience.info/journals/Article/SCAS/10460135.pdf.